

# Weierstraß-Institut für Angewandte Analysis und Stochastik

im Forschungsverbund Berlin e.V.

Preprint

ISSN 0946 – 8633

## The heat treatment of steel — A mathematical control problem

Dietmar Hömberg, Daniela Kern

submitted: February 9, 2009

Weierstrass Institute  
for Applied Analysis  
and Stochastics  
Mohrenstraße 39  
10117 Berlin  
Germany  
E-Mail: hoemberg@wias-berlin.de  
kern@wias-berlin.de

No. 1402  
Berlin 2009



---

2000 *Mathematics Subject Classification.* 74P10, 80A20, 93C20.

*Key words and phrases.* Laser surface hardening, optimal control, pyrometer control.

This work has been supported by the DFG Research Center MATHEON “Mathematics for key technologies” in Berlin.

Edited by  
Weierstraß-Institut für Angewandte Analysis und Stochastik (WIAS)  
Mohrenstraße 39  
10117 Berlin  
Germany

Fax: + 49 30 2044975  
E-Mail: [preprint@wias-berlin.de](mailto:preprint@wias-berlin.de)  
World Wide Web: <http://www.wias-berlin.de/>

## Abstract

The goal of this paper is to show how the heat treatment of steel can be modelled in terms of a mathematical optimal control problem. The approach is applied to laser surface hardening and the cooling of a steel slab including mechanical effects. Finally, it is shown how the results can be utilized in industrial practice by a coupling with machine-based control.

## 1 Introduction

The aim of this paper is to show that the natural mathematical description of the heat treatment of steel is given in terms of an optimal control problem. The desired goal is described by a cost functional. A typical choice would be

$$J(z, u) = \frac{1}{2} \int_{\Omega} |z(x, t_E) - \bar{z}(x)|^2 dx . \quad (1)$$

For a vector  $z = (f, p, b, m)$  of phase fractions of ferrite, pearlite, bainite and martensite,  $J(z, u)$  measures the distance between the actual phase distribution at end-time  $t_E$  and the desired one,  $\bar{z}$ , in the workpiece  $\Omega$ . The goal of the heat treatment then is to find an optimal control  $u^*$ , i.e., an optimal cooling strategy, such that  $u^*$  is the solution to the following control problem:

$$(CP) \quad \begin{cases} \min J(z, u) \\ \text{subject to equality constraints for temperature } T \\ \text{and phase fraction } z. \end{cases}$$

In the simplest case, the equality constraints are given by the heat equation and a system of rate laws for the phase fractions. The control parameter  $u$  could be the temperature of the coolant, the heat transfer coefficient or the power of a laser source.

In the next section, we describe a mathematical model for laser and electron beam hardening. In Section 3, we show how these planning of the beam treatments can be assisted by the solution of a corresponding control problem. The last section is devoted to some concluding remarks on future research.

## 2 A Model of Laser Surface Hardening

Figure 1 depicts the laser hardening process. A laser beam moves along the surface of a workpiece. The absorbed energy leads to a heating of the boundary layer followed by the formation of austenite. Typical penetration depth is less than one millimeter. Hence by self-cooling the desired martensite layer is produced.

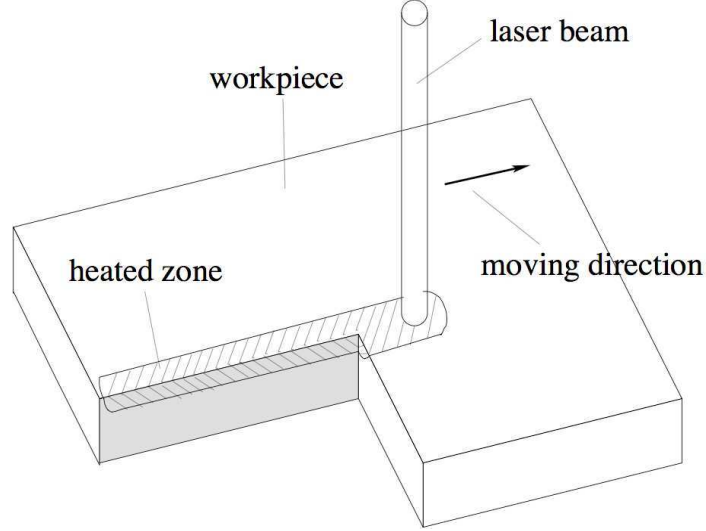


Figure 1: Sketch of laser hardening process.

The basic assumption for our phase transition model is that all the necessary information are constrained in the respective TTT, CCT, and austenitization diagrams. In particular, we do not strive for a model in which all parameters can be given a precise physical interpretation. Our aim is to develop a phenomenological model with sufficiently rich parameter structure, such that all the transformation diagrams can be reproduced well.

To be more precise, we define a temperature field  $T(x, t)$  with temporal derivative  $\dot{T}$  and  $a$  the phase fraction of austenite. The expression  $[u]_+ = \max \{0, u\}$  describes the positive part of a function  $u$ . The principal building block to describe the growth of a phase  $z$  is given by the following rate law:

$$\dot{z}(t) = z^{r(T)} [z_{eq}(T) - z]_+^{s(T)} g(T) h(\dot{T}).$$

Here,  $z_{eq}(T)$  denotes the equilibrium fraction for the phase  $z$  that will be attained asymptotically at fixed temperature  $T$ . In the case  $z_{eq} \equiv 1, r \equiv 0, s \equiv 1, h \equiv 1$  and  $g \equiv c$  with a positive constant  $c$ , one obtains a typical Avrami-Kolmogorov kinetics, i.e.,  $z(t) = 1 - (1 - z_0)e^{-ct}$ . In the case  $r \equiv 1, s \equiv 0, h \equiv 1$  and  $g \equiv 1$  one obtains the Leblond & Devaux model [Leblond, Devaux 1984].

Figure 2 depicts the phase transitions during laser hardening. The heating leads to a growth of austenite in a boundary layer. Upon cooling, it is mostly transformed to martensite. Depending on the workpiece geometry also smaller amounts of ferrite, pearlite, and bainite can be formed. We call these quantities  $f, p, b, m$ , relative volume fractions, which grow at the expense of the austenite formed during heating.

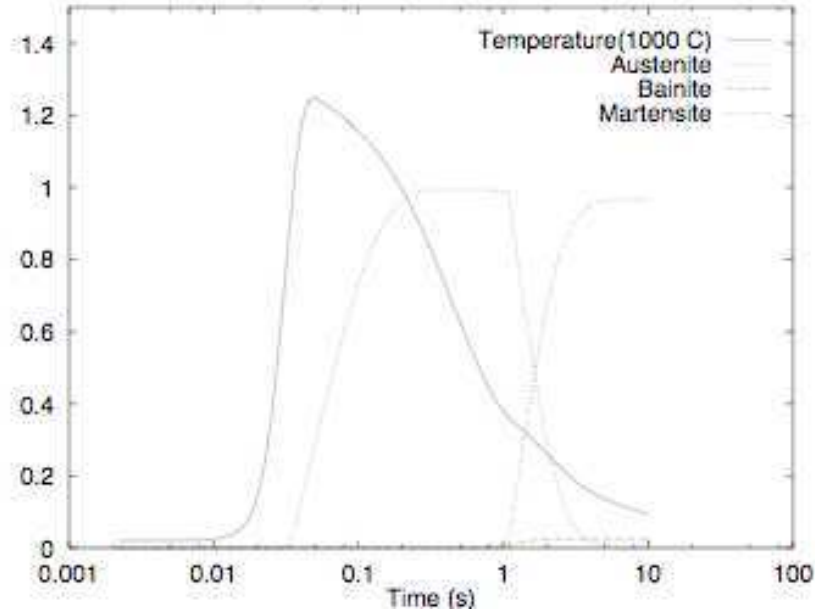


Figure 2: Temporal evolution of temperature and phase fractions in a fixed point in the workpiece.

A straightforward generalization of the previous equation yields the following model for the phase transitions during a complete heat treatment cycle:

$$\begin{aligned} a(0) = m(0) = 0, \quad f(0) = f_0 \\ p(0) = p_0, \quad b(0) = b_0 \end{aligned} \quad (2a)$$

$$\dot{a}(t) = \frac{1}{\tau_a(T)} [a_{eq}(T) - a]_+ \quad (2b)$$

$$\dot{f}(t) = f^{r_f(T)} [\tilde{f}_{eq}(T) - f]_+^{s_f(T)} g_f(T) h_f(\dot{T}) \quad (2c)$$

$$\dot{p}(t) = p^{r_p(T)} [\tilde{p}_{eq}(T) - p]_+^{s_p(T)} g_p(T) h_p(\dot{T}) \quad (2d)$$

$$\dot{b}(t) = b^{r_b(T)} [\tilde{b}_{eq}(T) - b]_+^{s_b(T)} g_b(T) h_b(\dot{T}) \quad (2e)$$

$$\dot{m}(t) = \frac{1}{\tau_m(T)} [\tilde{m}(T) - m]_+ \quad (2f)$$

(2a) is the Leblond & Devaux model for the growth of austenite. The equilibrium fraction  $a_{eq}$  is zero below and 1 above  $A_f$ , inbetween it grows monotonically. Hence, the growth of austenite starts when the temperature has reached  $A_s$ . Due to the projection on the positive part  $[\cdot]_+$ ,  $\dot{a}(t) = 0$  for decreasing temperature. Altogether,  $a(t)$  is a non-decreasing function, although in reality,  $a(t)$  is diminished by the growth of the product phases  $f, p, b, m$ .

At any time  $t$ , the fraction of ferrite, which can be attained maximally, is given as the sum of the fraction produced so far,  $f(t)$ , and the remaining fraction of austenite,  $a(t) - f(t) - p(t) - b(t) - m(t)$ . The same holds true for the other product phases. Hence, we define the functions  $\tilde{f}_{eq}, \tilde{P}_{eq}, \tilde{b}_{eq}, \tilde{m}_{eq}$  as

$$\tilde{f}_{eq}(T) = \min\{f_{eq}(T), a - p - b - m\} \quad (3a)$$

$$\tilde{P}_{eq}(T) = \min\{p_{eq}(T), a - f - b - m\} \quad (3b)$$

$$\tilde{b}_{eq}(T) = \min\{b_{eq}(T), a - f - p - m\} \quad (3c)$$

$$\tilde{m}(T) = \min\{m_{KM}(T), a - f - p - b\}. \quad (3d)$$

One should remark that non-zero initial conditions for  $f, p$ , and  $b$  are necessary to ensure unique solvability of the system (2a–f). The equilibrium fractions  $a_{eq}, f_{eq}, p_{eq}, b_{eq}$  can be derived from the respective TTT and austenitization diagrams. The function  $m_{KM}$  describes the fraction of martensite according to the Koistinen-Marburger formula [Koistinen, Marburger, 1959], i.e.,

$$m_{KM} = 1 - e^{-c_m(M_s - T)}$$

where  $c_m$  and  $M_s$  again can be drawn from the TTT diagram. The remaining data functions can also be identified from the TTT and CCT diagram of the respective steel using parameter identification tools [Buchwalder et al., 2002].

The temperature field is governed by the heat equation

$$\rho c(T) \dot{T} - \nabla \cdot (k(T) \nabla T) = q_1 + q_2. \quad (4)$$

The first heat source is due to recalescence effects of the phase transitions and can be written as

$$q_1 = \rho L \cdot \dot{z}$$

where  $z = (a, f, p, b, m)$  and  $L = (-L_a, L_f, L_p, L_b, L_m)$ , and  $L_a, \dots, L_m$  are the positive latent heats of the different phases. Since  $L_a$  is positive and  $\dot{a}$  is positive during the growth of austenite, we can infer  $-L_a \dot{a} \leq 0$ , i.e., latent heat is consumed during the formation of austenite, while it is released during the growth of the product phases.

The second heat source  $q_2$  describes the absorption of laser energy. For ease of presentation, we restricted ourselves here to the case of a flat workpiece boundary lying in the plane  $z = 0$  such that the rest of the boundary is in the half space  $z \leq 0$ . Then, we can define

$$q_2 = P(t)\eta F(x - \gamma_1(t), y - \gamma_2(t))e^{-\kappa z} \quad (5)$$

as a volumetric laser heat source, decaying exponentially with growing distance from the impinged surface, since  $\kappa$  is a positive constant. In the sequel, the laser power  $P(t)$  will serve as a control parameter,  $\eta$  is the absorption coefficient, and  $F(x, y)$  a normalized radiation profile (cf. Figure 3). The path of the laser on the workpiece is parameterized by  $\gamma(t) = (\gamma_1(t), \gamma_2(t))$ .

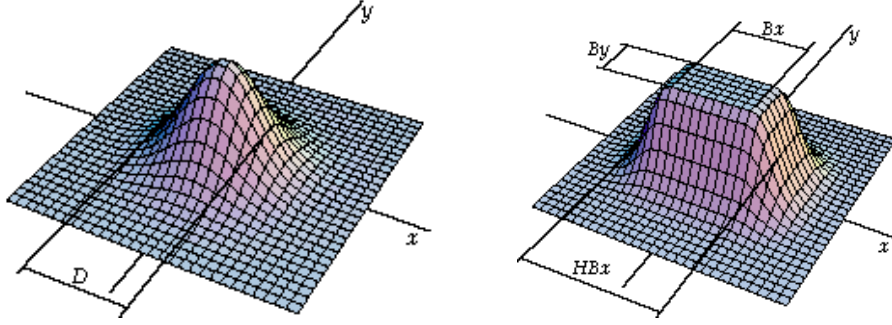


Figure 3: Radiation profiles for gas (left) and Nd:YAG laser (right).

The complete model of laser surface hardening consists of the coupled system (2)–(5). A particular mathematical difficulty lies in the nonlinearities in  $\dot{T}$ . However, in [Hömberg, 1997] it has already been shown that a system with a similar structure admits a unique solution.

For the numerical solution of this system the software WIAS-SHarP has been developed. To cope with the difficulty that the phase transition occur only in a boundary layer which is small compared to the workpiece dimension, the heat equation is solved on an adaptive grid. This allows a refinement of the grid around the laser focus, whereas the grid is coarser where the temperature has already decreased. The phase transitions are solved on different grid which is homogeneously refined along the trace of the laser. Figure 4 depicts the temperature distribution and the corresponding grid for two different simulation times.

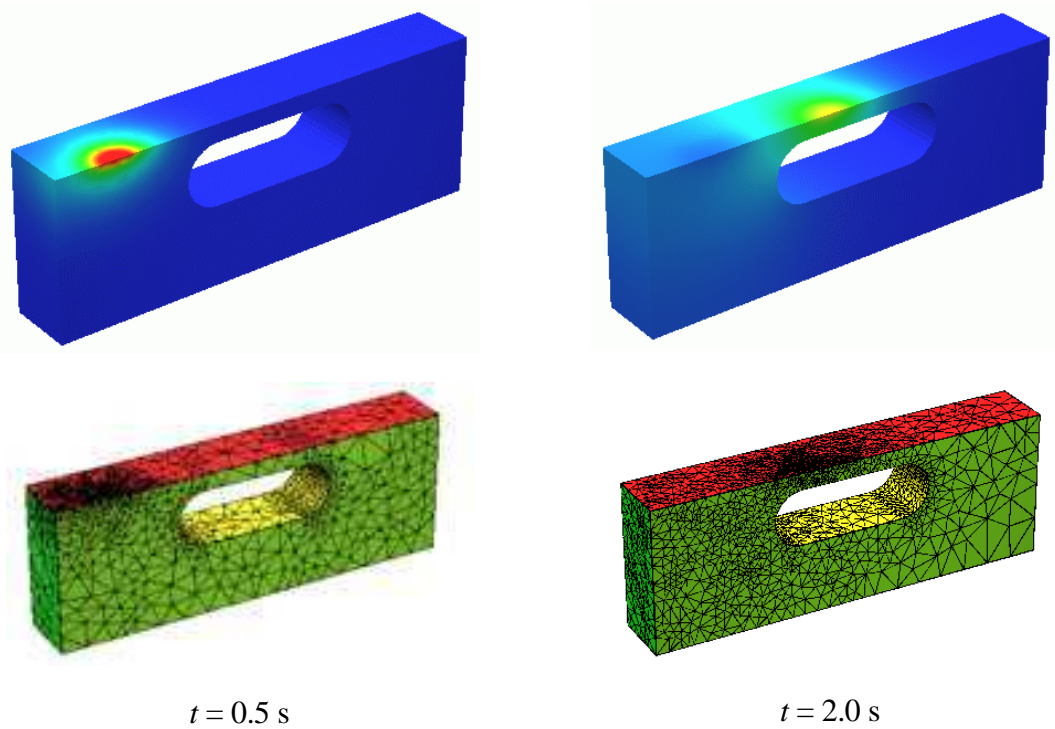


Figure 4: Temperature distribution and adaptive grid at two different times.

Figure 5 depicts a screenshot of WIAS-SHarp. Its GUI enables a comfortable input of treatment parameters and allows for an efficient online graphical visualization.

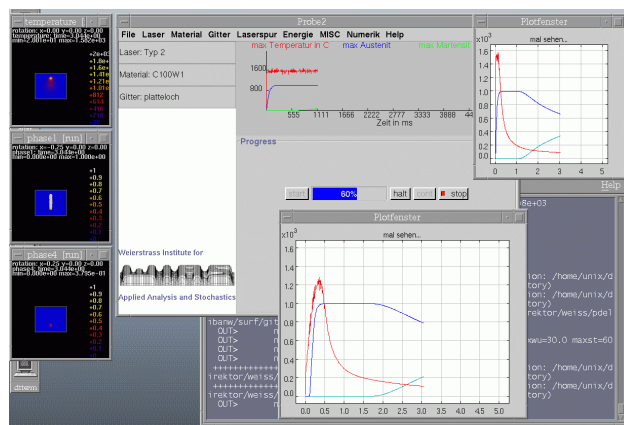


Figure 5: Screenshot of WIAS-SHarp.

### 3 Optimal Control of Heat Treatments

#### 3.1 Temperature control

Figure 6 shows the results of laser hardening with constant laser power and constant feeding velocity. As one can see, over-heating at edges and above cavities leads to the undesired effect of



surface melting. To simplify the exposition, we restrict ourselves for a moment to the temperature field. From mathematical point of view, the task is to find an optimal laser power  $P^*(t)$  such that  $|T(x,t) - \bar{T}(x)|$  is small in a neighbourhood  $B(\gamma(t))$  of the laser focus on the surface.  $\bar{T}(x)$  is the desired temperature and the curve  $\gamma(t)$  describes the laser track on the surface. In other words, we want to minimize the cost functional

$$J(P) = \frac{1}{2} \int_0^{t_E} \int_{\Omega} \omega(T - \bar{T})^2 dx dt + \frac{\alpha}{2} \int_0^{t_E} P^2 dt,$$

where the weight  $\omega(x,T) = 1$ , if  $(x,t)$  is in  $B(\gamma(t))$  and  $\omega(x,t) = 0$ , else. The second term is a regularization term penalizing high costs. The control problem then is to minimize this cost functional while  $T(x,t)$  satisfies the heat equation with heat source according to (5).

The numerical solution of such a problem requires several iterations in which the time-dependent heat equation, as well as a so-called adjoint equation have to be solved. Figure 7 shows the results of the numerical solution of the problem.

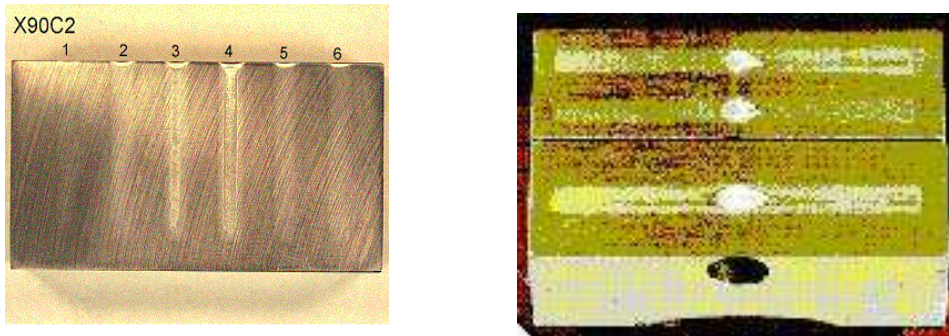


Figure 6: Melting at edges and above cavities.

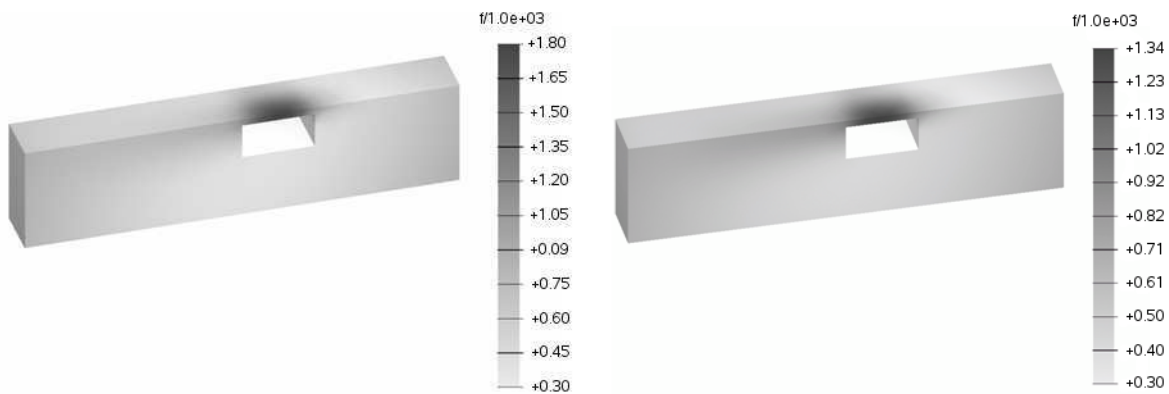


Figure 7: Initial and optimal temperature distribution above the cavity.

On the left one can see the initial solution at the time when the laser crosses the cavity, on the right the solution after 16 iterations is depicted. Both simulations look similar, however, the scale reveals that the temperature above the hole is 1800 K in the initial iteration while it is just 1340 K in the final iteration.

### 3.2 Control of microstructure

The simplest model to describe the effect of distortions due to heat treatments is a coupling between the phase system (2.a-f) and the equations of quasi-static linearized thermoelasticity, where the coupling is realized by a temperature dependent thermal expansion. We consider a cooling process from the austenite. As a control parameter we can choose the thermal exchange coefficient  $\alpha$  in the Newton cooling law

$$-k \frac{\partial T}{\partial n} = \alpha(T - T_{ext}).$$

Here,  $T_{ext}$  is the temperature of the coolant. To demonstrate the distortion due to phase transitions we consider a two-dimensional simulation of the cooling of a steel slab from below (cf. Figure 8). At  $t = 0s$ , the specimen is homogeneously austenitic, after 20s due to cooling at the lower boundary one can observe a downward bending. Finally, after 100s the specimen has nearly reached room temperature and one can observe a remaining upward bending due to the creation of martensite in the bottom layer of the specimen.

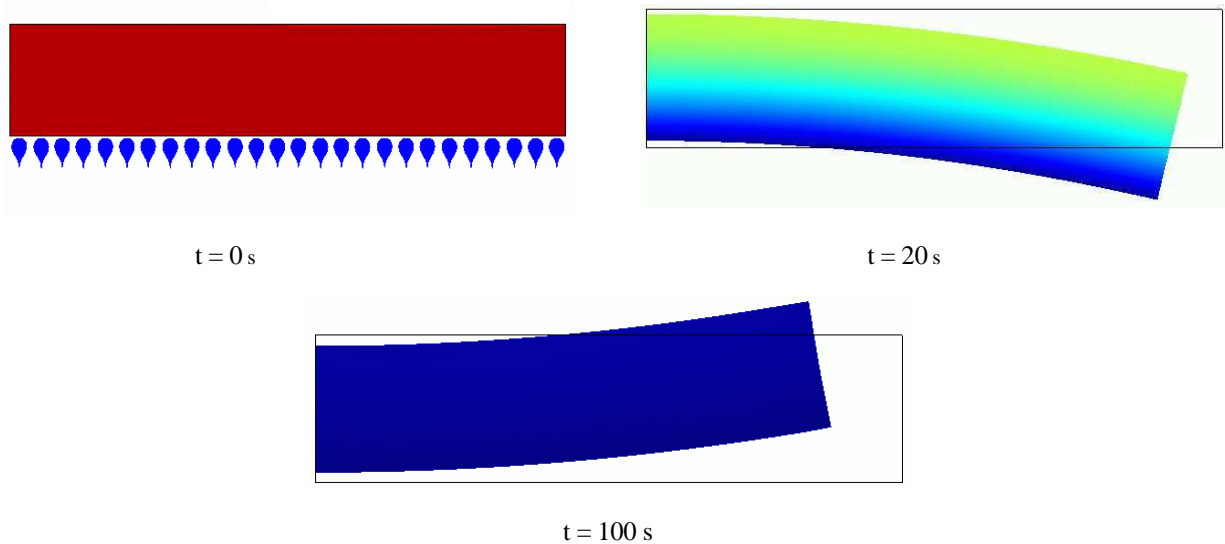


Figure 8: Distortion due to cooling.

Now we consider the corresponding control problem. We take a cost functional similar to (1), but using now the heat exchange coefficient  $\alpha$  as a control. Figure 9 depicts the initial (left) and the desired microstructure (right), which is used to define the desired phase distribution  $\bar{z}$  in the cost functional.

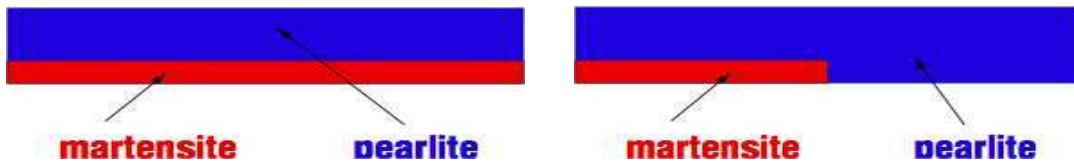


Figure 9: Initial (left) and desired microstructure (right).

Figure 10 shows 5 iterations of the gradient method for the solution of the optimal control problem. Note that each picture is the result of a complete solution of the state system and the adjoint system. One can see how by a cooling along the complete lower boundary of the specimen first the initial phase distribution is created and then the desired phase profile is approximate more and more closely in the course of the iterations.

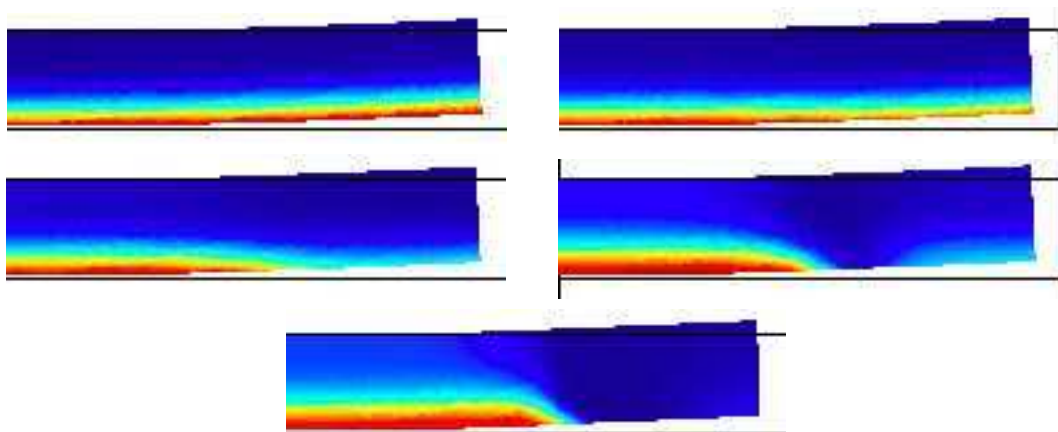


Figure 10: Five iterations of the gradient method.

### 3.3 Interplay with machine-based control

The question that arises now is, how one can utilize the results of such an optimization process in industrial practice. Very often, not all the necessary parameters are known, in laser hardening for instance, it is nearly impossible to predict the actual absorption coefficient for the laser light, which impinges the surface. In [Hömberg, Weiss, 2006], [Alder, Hömberg, Weiss, 2006] we have shown how the results can be used in combination with a machine based process control. To this

end the optimal laser power is first used to compute the optimal temperature in the laser beam focus. The latter then serves as a set-point for the machine based control. Figure 11 illustrates this procedure for the surface hardening above a cavity. The goal is to achieve a constant hardening depth. Figure 11 (left) depicts the computed optimal temperature in the laser focus. Then this temperature is used as the set-point for the machine based control. The picture on the right shows that this strategy indeed yields the desired constant hardening depth.

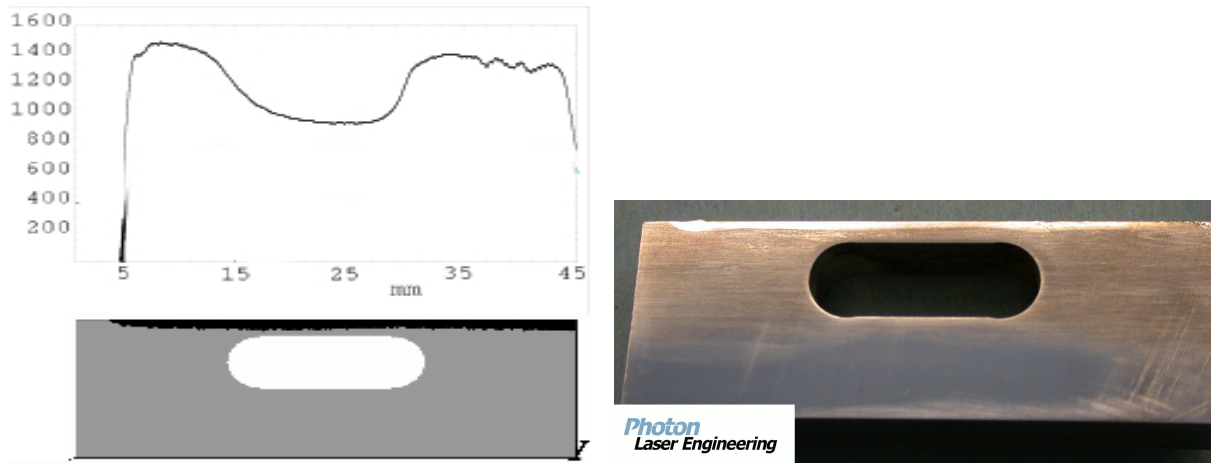


Figure 11: Optimal temperature in the laser focus and resulting simulated martensite depth (left), experimentally achieved hardening depth (right).

## 4 Conclusions

The goal of this contribution was to demonstrate how the heat treatment of steel can be described mathematically in terms of an optimal control problem. Its numerical simulation requires several iterations of the solution of the field equations and adjoint equations. However, this effort is mitigated by the development of new model reduction strategies allowing for the efficient computation of a solution within reasonable time [Hömberg, Volkwein, 2003].

A challenging direction of research is to treat the task of distortion engineering as an optimal control problem. Here, investigations branch into two directions. The first is optimal control of phase transitions to compensate distortion, e.g., to minimize the out-of-roundness of roller bearing rings [Hömberg, Kern, 2008]. This topic is subject of actual investigations in a cooperation between IWT and WIAS. The second direction is to find an appropriate initial shape of the workpiece in order to compensate distortions caused by subsequent heat treatments. Mathematically, this requires the solution of an optimal shape design problem and is a challenging task for future research.

## References

- Alder, H., Hömberg, D., Weiss, W.: Simulationsbasierte Regelung der Laserhärtung von Stahl. HTM Z. Werkst. Wärmebeh. Fertigung, 61 (2006), pp. 103-108.
- Buchwalder, A., Hömberg, D., Jurke, Th., Spies, H.-J., Weiss, W.: Simulation der Strahlhärtung von Stahl mit WIAS-SHarP. WIAS, Tech. Report 3, Berlin, 2002.
- Hömberg, D.: Irreversible phase transitions in steel. Math. Methods Appl. Sci., 20 (1997), pp. 59-77.
- Hömberg, D., Kern, D.: The heat treatment of steel – A mathematical control problem, in: H.-W. Zoch, Th. Lübben (eds.), Proceedings 2<sup>nd</sup> International Conference on Distortion Engineering, Bremen, September 17 – 19, 2008, IWT Bremen, 2008, pp. 201-209.
- Hömberg, D., Volkwein, S.: Control of laser surface hardening by a reduced-order approach using proper orthogonal decomposition. Math. Comput. Modelling, 38 (2003), pp. 1003-1028.
- Hömberg, D., Weiss, W.: PID control of laser surface hardening of steel. IEEE Trans. Control Syst. Technol., 14 (2006), pp. 896-904.
- Koistinen, D., Marburger, R.: A general equation prescribing the extent of the austenite-martensite transformation in pure iron-carbon alloys and plain carbon steels. Acta Met., 7 (1959), pp. 59-60.
- Leblond, J.-B., Devaux, J.: A new kinetic model for anisothermal metallurgical transformations in steels including effect of austenite grain size. Acta Met., 32 (1984), pp. 137-146.